Audio-Based Telemetry Using HT Radios for Remote Monitoring of Renewable Energy Systems

Sigit Dani Perkasa [1], Ahmad Rahmad Muzadi [2], Prisma Megantoro [3,*], Vighneshwaran Pandi [4]
[1,2,3] Faculty of Advanced Technology and Multidiscipline, Universitas Airlangga, Surabaya, Indonesia
[4] Department of Computer Science and Engineering, Acharya University, Karakul, Uzbekistan
Email: [1] sigit.dani.perkasa-2020@ftmm.unair.ac.id, [2] ahmad.rahmad.muzadi-2020@ftmm.unair.ac.id,
[3] prisma.megantoro@ftmm.unair.ac.id, [4] vigneshwaran31@acharya.ac.uz
*Corresponding Author

***Abstract*—Effective monitoring of renewable energy systems, such as wind turbines and photovoltaic arrays, is essential for optimizing energy production. However, traditional wired monitoring systems are expensive and lack flexibility. This study develops a reliable wireless monitoring system that addresses the limitations of wired alternatives, using a PZEM-004T power meter, Arduino Uno R3, and BF-888S HT radios. The system employs audio-modulated binary encoding for long-range, low-cost data transmission, enabling real-time monitoring of key power parameters, including voltage, current, and power factor. This solution offers scalability and cost-effectiveness by eliminating the need for extensive infrastructure. The methodology involves designing both hardware and firmware for the transmitter and receiver components and developing a communication algorithm to optimize data transfer efficiency. The system was tested in various environments: indoor, outdoor, and radio communication scenarios. Performance varied across environments, with outdoor and higher-floor tests experiencing more significant interference, which impacted transmission quality. The system achieved an average transmission time of 42.64 seconds and an error rate of 0.56% across 16 channels, demonstrating competitive reliability compared to existing wireless systems. Future research could explore adaptive modulation techniques to enhance data reliability in high-interference environments, improving the system's robustness for large-scale deployments.**

Keywords*—*Audio-Modulated Encoding, Data Transmission, Power Monitoring, Radio Telemetry, Renewable Energy Monitoring, Wireless Monitoring

I. INTRODUCTION

Efficient monitoring of renewable energy systems, such as wind turbines and photovoltaic arrays, is essential for optimizing energy production and ensuring grid stability. However, traditional wired monitoring systems are costly and inflexible, limiting their scalability and complicating the management of large installations. These systems also face challenges in installation complexity, maintenance, and data transmission reliability, which can hinder the effective monitoring of remote or distributed energy sources.

Recent research has explored wireless telemetry solutions for real-time monitoring of key power parameters, such as voltage, current, and power factor [1], [2]. IoT-based technologies and power factor correction methods have shown promise in improving system performance, particularly in remote environments [3], [4]. However, existing solutions still suffer from limitations related to range, cost, and the need for extensive infrastructure, creating a gap for more efficient and scalable approaches. This paper proposes a novel wireless telemetry system integrating a PZEM-004T power meter, Arduino Uno R3, and BF-888S HT radios. This system uses audio-modulated binary encoding for reliable long-distance data transmission, offering enhanced performance compared to existing wireless solutions. The choice of components was driven by their cost-effectiveness, accuracy, and range, making them ideal for large-scale renewable energy monitoring. The proposed system provides a scalable, low-cost solution that improves monitoring efficiency, especially in large, distributed installations [5], [6].

II. METHOD

A. System Design

The system designed in this research is illustrated in Fig. 1. The system represents a hybrid renewable energy monitoring setup, integrating wind turbines and photovoltaic (PV) arrays connected to the electrical grid.

The system configuration diagram in Fig. 1 shows the PZEM-004T power meter, which measures power parameters and is processed by an Arduino Uno R3. The data is transmitted wirelessly using BF-888S HT radios to another BF-888S HT unit, which forwards the information to an Arduino Uno WiFi Rev2. This final microcontroller uploads the collected data to a remote database for storage and analysis, enabling remote monitoring of energy production and consumption [7]-[10]. BF-888S was chosen because it offers several advantages for radio communication over other technologies like LoRa, Zigbee, and RF. One significant benefit is their versatility in different communication environments, with their simple and direct transmission [11].

B. Telemetry Device Integration

1) Hardware Integration

The proposed system's hardware integration, which consists of a transmitter and a receiver, is explained in the schematic diagram in Fig. 2.

Fig. 2 explains the schematic of the proposed telemetry system, whereas Fig. 2 a for the transmitter and Fig. 2 b for the receiver. The transmitter system utilizes a PZEM sensor with a Current Transformer (CT) to measure power, connected serially to pins 2 and 3 of an Arduino Uno R3. The microcontroller processes the measured values and converts the data into an audio signal for transmission. The output to HT includes three resistors: R1 and R3 limit the current flow

to the HT on pins 12 and 13, while R2 acts as a voltage drain to prevent interference signals. The receiver system (Fig. 1 b) receives data via the HT input. The audio signal from the HT speaker output is filtered using a 300-ohm resistor and coupled with a 1 µF electrolytic capacitor (elko) before being fed into a comparator module. The comparator compares the input signal with a reference voltage and outputs a digital high or low signal, depending on whether the input signal is above or below the reference. The comparator's output is further filtered using a 4.7 µF electrolytic capacitor before being transmitted to pin 2 of an Arduino Uno WiFi Rev2. The digital signal is then processed, displayed, and transmitted to Firebase for remote monitoring and analysis.

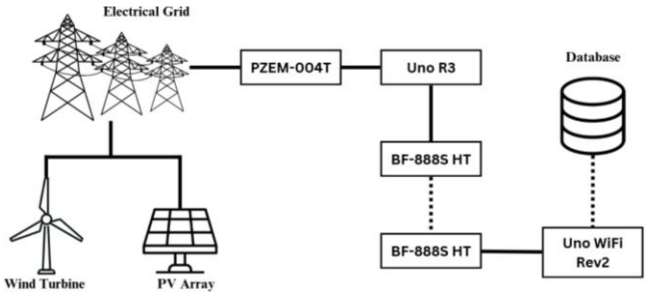

Fig. 1. System configuration diagram

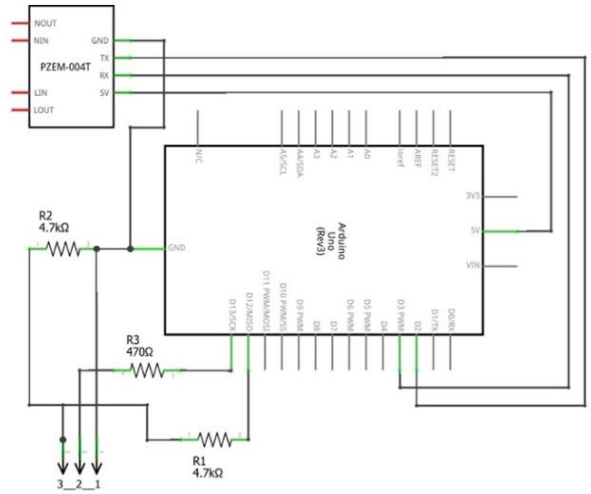

(a)

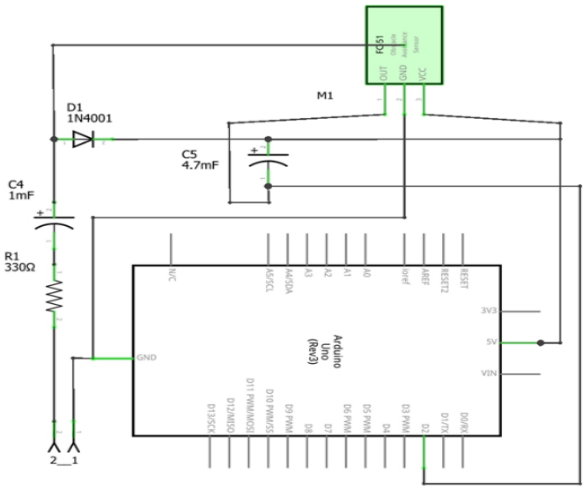

(b)

Fig. 2. Schematic of the telemetry system, (a) transmitter and (b) receiver

2) *Firmware Design*

The proposed telemetry system's firmware design is divided into two parts: receiver and transmitter. The workflow of both parts is explained in the flowcharts in Fig. 3.

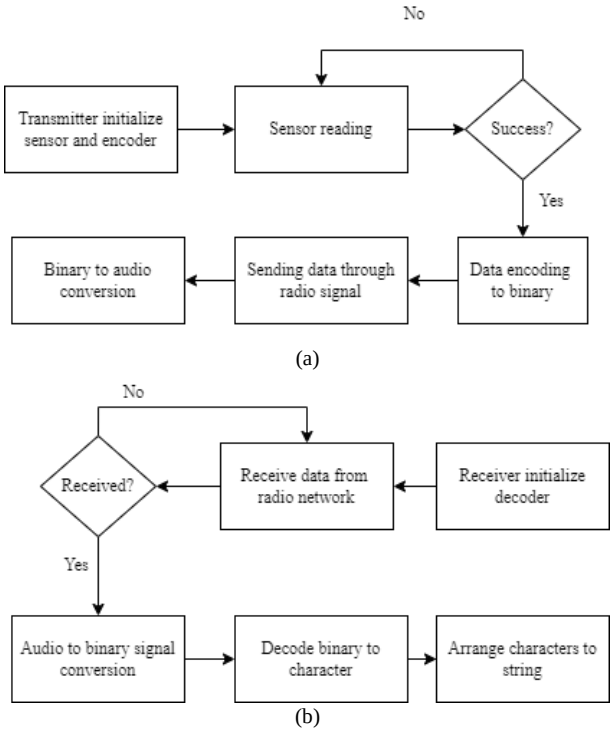

Fig. 3. Firmware workflow of the telemetry system, (a) transmitter and (b) receiver

The telemetry system firmware in Fig. 3 consists of the transmitter in Fig. 3 a and the receiver in Fig. 3 b. The transmitter firmware initializes the sensor and encoder. It reads power data from the PZEM sensor and current transformer (CT) and encodes it into a binary format. This binary data is then converted into an audio signal for transmission. The audio signal is sent to the receiver via Handy Talky (HT) radios over a radio network. On the receiver side (Fig. 3 b), the system initializes the decoder and listens for incoming data. Once received, the audio signal is converted into binary, decoded into characters, and arranged into a string. The processed data is then displayed on a local interface or sent to Firebase for remote monitoring.

The system implements error-checking measures to ensure data integrity during transmission. When a packet is received, the system checks for any transmission errors, such as signal distortion or packet loss. If the data is corrupted, the receiver requests a retransmission of the lost or corrupted packet. The system also uses checksums to verify the accuracy of the data, ensuring that the decoded string matches the expected format.

C. *Communication Algorithm*

The communication algorithm in the proposed system is divided into transmitter and receiver functions.

1) *Transmitter*

The transmitter function encodes numerical and special character data into an audio-based binary modulation scheme for transmission via HT. The encoding involves tone

generation, binary mapping, and time delay management to ensure accurate data transmission.

a) Tone signal generation

A series of 700 Hz tones were generated based on an 8-bit binary input, where each bit determines the tone duration. The tone modulation follows the rule:

$$T_i = \begin{cases} Tone(700,100) + Delay(50), if\ val_i = 1 \\ Tone(700,50) + Delay(50), if\ val_i = 0 \end{cases} \quad (1)$$

for *i = 1, 2, ..., 8*. *Tone(700, x)* denotes a 700 Hz tone lasting for *x* milliseconds. This frequency helps achieve better spectral efficiency and reduced computational demands, leading to more energy-efficient designs. 700 Hz performs well in noisy environments, providing a more reliable and clearer signal, which is essential for maintaining communication quality while conserving battery life [12]. The frequency also ensures optimal energy efficiency by balancing communication reliability and power consumption, crucial for devices that require continuous operation [13], [14]. Furthermore, its selection aligns with the need for low-power transceiver systems that efficiently manage resources without compromising audio clarity [15]. The selection of 50ms delays in the tone modulation system is supported by considerations of energy efficiency and communication reliability. Studies indicate that minimal delays, such as 50ms are crucial for maintaining low-latency communication in energy-efficient systems, which is essential in noisy environments where signal clarity is paramount [16]. Additionally, the function includes a transmission delay factor:

$$\Delta_t = \begin{cases} 95ms, & if\ tm = 1 \\ 0ms, & if\ tm = 0 \end{cases} \quad (2)$$

Incorporating transmission delays like 95ms ensures reliable synchronization while reducing computational demand, a critical factor in resource-constrained designs [17]. Thus, the total transmission duration for a single-tone sequence is:

$$T_{total} = \sum_{i=1}^{8} T_i + \Delta_t \quad (3)$$

This formulation ensures that each binary value is consistently modulated into an audio waveform for transmission.

b) Binary encoding of characters

The binary encoding technique used in tone modulation systems, where the comparator function outputs a digital signal, is similar to on-off keying (OOK) or binary linear modulation. In such systems, the analog input tone is compared against a reference to generate a binary output, which efficiently encodes information in noisy environments while minimizing errors and reducing the complexity of the design [18], [19].

Each alphanumeric character is mapped to a corresponding 8-bit binary sequence, followed by the *tm* delay parameter. The mapping can be expressed as:

$$C_x = (b_1, b_2, b_3, b_4, b_5, b_6, b_7, b_8, tm) \quad (4)$$

Where C_x represents the binary encoding for character *x*. The firmware retrieves the predefined binary sequence for each character and passes it as a parameter to the function. For example, the character '1' is mapped as follows:

$$C_x = (0,0,1,1,0,0,0,1,1) \quad (5)$$

which translates into tone sequence:

$$T_3 + T_4 + T_5 + \Delta_t \quad (6)$$

Each character is uniquely represented in the audio domain, allowing accurate transmission and decoding on the receiver side.

c) Transmission timing model

The transmission function iterates over a string S of length N, encoding each character sequentially. Before each transmission, the push-to-talk (PTT) pin is activated, introducing a fixed 650ms delay to stabilize the transmission. The total transmission time for a string S is:

$$T_{transmit} = N \times (T_{total} + 650 + T_{PTT} \quad (7)$$

Where T_{PTT} represents the time required for PTT activation and deactivation.

2) Receiver

The receiver function decodes audio-modulated binary data transmitted from the sender via HT. The system captures, processes, and interprets the original digital data by detecting signal patterns and extracting meaningful values. The input pin of the HT is continuously read to detect incoming binary signals. The detection logic follows these conditions:

$$B_t = \begin{cases} 1, & if\ input = LOW\ for\ a\ long\ T_{press} \\ 0, & otherwise \end{cases} \quad (8)$$

Where B_t represents the detected binary value at time *t*. T_{press} or button activation time is tracked using:

$$T_{press} = millis() - 5ms \quad (9)$$

If T_{press} exceeds a long press threshold of 75ms, the input is considered as '1' and otherwise it is classified as '0'. The received binary sequence is stored in an array and indexed accordingly. To proper sequence reconstruction and dynamic updates, the system manages state transition using:

$$B_{active} = \begin{cases} True, & if\ signal\ detected \\ False, & if\ no\ signal\ detected \end{cases} \quad (10)$$

D. Testing Methodology

This study's testing scenario is divided into three parts: basic data transmission, outdoor testing, and indoor testing. The tests were evaluated by calculating the transmission errors for each test scenario. The error calculation is represented in Equation (11).

$$E(\%) = \frac{|\text{Received Binary} - \text{Transmitted Binary}|}{\text{Transmitted Binary}} \times 100\% \quad (11)$$

Where E is the error rate of each transmission. This equation quantifies the discrepancy, providing insights into the system's transmission ability under varying scenario [20], [21].

III. Results and Discussion

A. Telemetry System

After a series of design and implementation, the next step is to test the device's communication to ensure the system's functionalities. The first test is to test the data transmission, presented in Fig. 4.

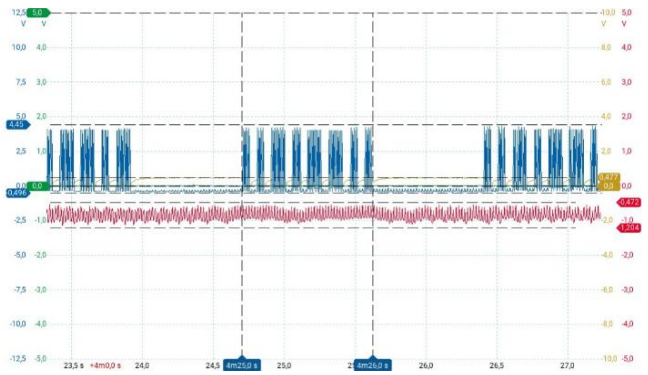

Fig. 4. Transmission and data signal for each transmission

Fig. 4 illustrates the signal testing results for data transmission in the electricity distribution telemetry system. The blue waveform represents the transmitted data signal, while the red waveform corresponds to the radio signal. In encoding, data is transmitted in binary format and converted into an audio signal at 700 Hz, with distinct time intervals for each bit. An audio frequency of 700 Hz is chosen because it generates clearer sound on a carrier signal with high noise levels, using a frequency that minimizes strain on electronic components, thus allowing for more efficient power consumption to produce sufficiently loud audio within the human hearing range, as the primary function of a handheld transceiver (HT) is audio communication.

The transmission time varies depending on the binary sequence, as binary '1' and '0' are differentiated by a 50ms signal interval per bit. Consequently, longer data sequences result in extended transmission durations. Based on signal testing, the average transmission time per data set is approximately 40.21 seconds. While acceptable for periodic updates, this delay could be too slow for applications needing rapid decision-making, such as detecting faults or fluctuations in energy production.

The transmitted data consists of three parameters: voltage, current, and power factor, all converted using the same method. Each data set begins with the character "S" and ends with "X" and uses a comma (',') as a delimiter to separate individual parameters, as presented in Table 1, Table 2, Table 3.

Table 1, Table 2, Table 3 presents the binary data transmission data translation for the telemetry system's voltage, current, and power factor parameters. Each parameter is encoded using 8-bit binary data with a stop bit (1-bit) at the end of each sequence. The binary values are then converted into decimals representing the measured electrical parameters. In Table 1, the voltage parameter is transmitted as multiple 8-bit binary segments, followed by a stop bit, and subsequently converted into its decimal representation, resulting in a final translated value of 228.30 V. Similarly, Table 2 illustrates the transmission of the current parameter, where the binary data sequence is processed and decoded into 0.45 A. Table 3 encodes the power factor parameter similarly, yielding a final translated value of 0.83. These results demonstrate the accuracy and consistency of the telemetry system in encoding, transmitting, and decoding electrical measurement data. The structured approach ensures that each transmitted dataset follows a standardized format, with a start character ("S"), comma-separated values, and an end character ("X"), facilitating efficient data parsing and processing.

Table 1. Voltage parameter data transmission and data translation

Param.	Data Type	Value	
Voltage	Bin.	001100101 001100101 001110001 001011111 001100111 001100001	
		8-Bit Data	00110010
		1- Stop Bit	1
	Dec.	Data	2
		Total Data	228.30
Translated Data		228.30	

Table 2. Current parameter data transmission and data translation

Param.	Data Type	Value	
Current	Bin.	001100001 001011111 001101001 001101011	
		8-Bit Data	00110100
		1- Stop Bit	1
	Dec.	Data	4
		Total Data	0.45
Translated Data		0.45	

Table 3. Power Factor parameter data transmission and translation

Param.	Data Type	Value	
Power Factor	Bin.	001100001 001011111 001110001 001100111	
		8-Bit Data	00111000
		1- Stop Bit	1
	Dec.	Data	8
		Total Data	0.83
Translated Data		**0.83**	

B. Radio Communications on Telemetry Device

After the device was operational, additional tests were conducted to assess data transmission from the transmitting to the receiving radio. The first test involved transmitting data for 30 minutes across 16 channels with a consistent distance parameter, aiming to evaluate transmission reliability and identify any significant interference that could affect data quality. The tested frequency channels are explained in Table 4.

Table 4 presents essential information on data transmission via radio channels, detailing 16 different radio channels, including frequency, codec, and tone specifications.

Table 4. HT BF-888S radio channel specification

Channel	Frequency (Hz)	Codec	Tone
CH1	462.125	CTCSS	69.3 Hz
CH2	462.225	-	-
CH3	462.325	-	-
CH4	462.425	CTCSS	103.5 Hz
CH5	462.525	CTCSS	114.8 Hz
CH6	462.625	CTCSS	127.3 Hz
CH7	462.725	CTCSS	136.5 Hz
CH8	462.825	DCS	162.2 Hz
CH9	462.925	DCS	D025N.
CH10	463.025	DCS	D051N.
CH11	463.125	DCS	D125N.
CH12	463.225	DCS	D1551.
CH13	462.525	DCS	D4651.
CH14	450.225	DCS	D023N.
CH15	460.325	-	-
CH16	469.945	CTCSS	203.5 Hz

The relationship between the codec, frequency, and tone in the HT BF-888S radio channels, as outlined in Table 4, is fundamental for effective communication and signal processing. The frequency refers to the specific radio channel on which the communication occurs, with each channel assigned a unique frequency (e.g., 462.125 MHz for CH1, 462.225 MHz for CH2). The codec specifies the modulation or encoding method used on the signal to allow communication over that particular frequency. For instance, channels with CTCSS (Continuous Tone-Coded Squelch System) or DCS (Digital Coded Squelch) codecs use specific tone frequencies to encode and filter signals, ensuring that only devices with the correct tone will transmit and receive on that channel.

The tone acts as a frequency that is used for subaudible signaling or squelch control. For example, channels with CTCSS, such as CH1 (69.3 Hz) and CH4 (103.5 Hz), require these tones to be transmitted along with the voice signal, ensuring that only radios tuned to the same tone can communicate. On the other hand, channels with DCS use digital codes (e.g., D025N on CH9) to similarly filter and enable communication between radios configured with matching codes. The tone and codec together define the access control mechanism for each channel, facilitating selective communication while minimizing interference from unrelated transmissions. Based on the channel information in Table 4, communication tests were conducted on the telemetry system, with the average results presented in the graphs in Fig. 5.

Fig. 5 displays the communication test results of the telemetry device, with transmission times (in seconds) in Fig. 5 a and corresponding error rates in Fig. 5 b both for 16 distinct channels. Transmission times range from a minimum of 32.11 seconds (channel 14) to a maximum of 51.27 seconds (channel 11), with most channels showing transmission times close to 42 seconds. The error rates vary between 0.00% and 2.98%, with channel 2 exhibiting the highest error rate of 2.98%, followed by channel 13 at 1.19%, and channel 14 at 1.15%. Conversely, channels 6 and 16 have the lowest error rates at 0.00%, indicating flawless transmission. The average transmission time across all channels is 42.64 seconds, while the average error rate is 0.56%.

C. Outdoor Test

The data transmission test was conducted outdoors over varying distances, with distance intervals of 50 meters. The test was performed up to a straight-line distance of 500 meters, illustrated in Fig. 6.

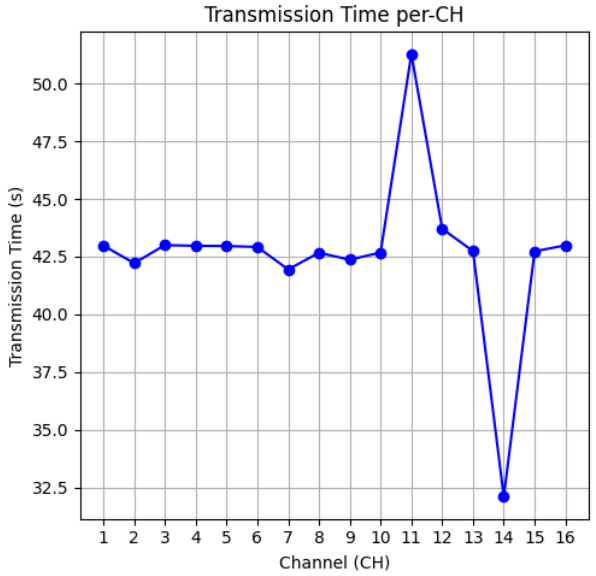

(a)

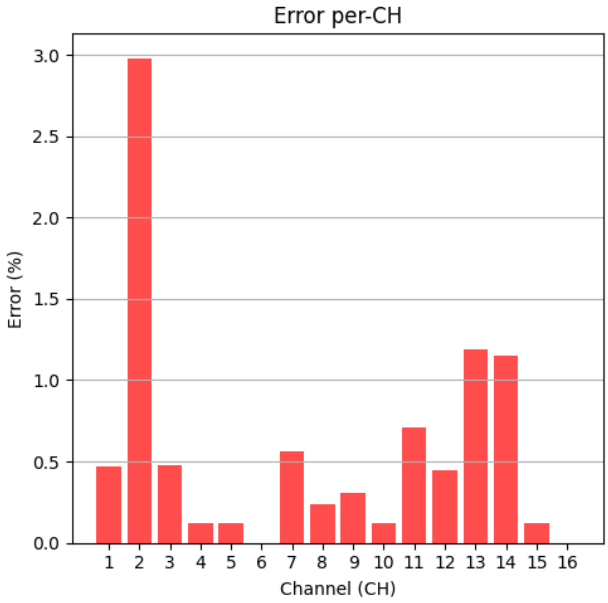

(b)

Fig. 5. Communication test on each radio channel, (a) Transmission time and (b) Transmission error

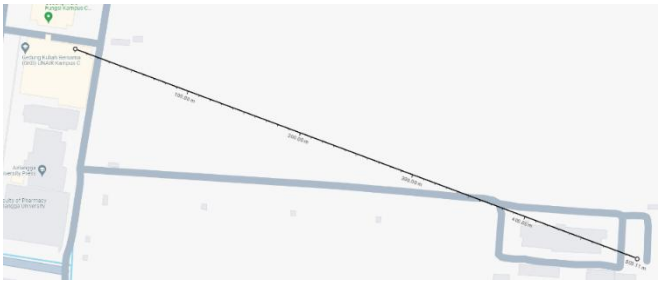

Fig. 6. Outdoor testing distance

This test evaluates the reliability of data transmission through various obstacles in the field and assesses the extent to which interference may affect data quality. The average results of the outdoor distance tests are presented in the graphs in Fig. 7.

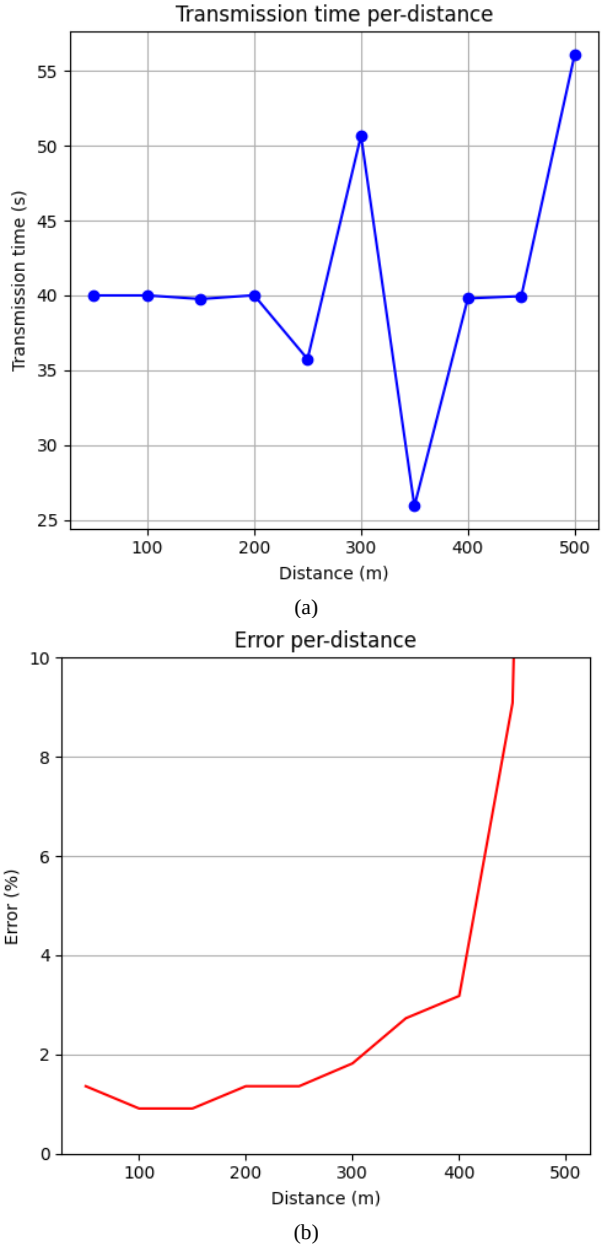

Fig. 7. Outdoor test results, (a) Transmission time and (b) Transmission error

Fig. 7 presents the outdoor testing results, where transmission times (in seconds) in Fig. 7 a and error rates in Fig. 7 b for data transmission across various distances, ranging from 50 to 500 meters. Transmission times generally remain close to 40 seconds for distances up to 250 meters, with some fluctuations, such as a significant increase at 300 meters (50.66 seconds) and 350 meters (25.94 seconds). The error rates increase with distance, starting at 1.36% for 50 meters and gradually rising, reaching a peak of 52.73% at 500 meters. The average transmission time across all distances is 40.80 seconds, with an average error rate of 7.55%, indicating a notable decline in transmission quality, especially at longer distances. This decline in transmission quality can be attributed to the increased distance, which causes signal attenuation and interference from other wireless signals, including Wi-Fi, Bluetooth, and nearby radio frequency sources. These factors contribute to signal degradation and a higher error rate at greater distances.

D. Indoor Test

Third, a data transmission test was conducted indoors, with varying distances based on approximately 3-meter vertical intervals corresponding to the number of floors in the NANO building at UNAIR Campus C. The test was performed up to a straight-line vertical distance of about 30 meters. This test aimed to assess the reliability of data transmission through various indoor obstacles, particularly floor differences, and to evaluate how interference impacts data quality. The average results of the indoor distance tests are presented in the graphs in Table 5.

Table 5. Indoor Test Results

Level	Transmission time (s)	Error rate
1	39.91	0.00%
2	39.93	0.45%
3	39.92	0.91%
4	40.74	0.45%
5	40.58	0.00%
6	39.92	0.00%
7	40.28	0.00%
8	39.97	0.45%
9	40.56	21.15%
10	586.01	43.33%
Average	**94.78**	**6.68%**

Table 5 presents the transmission times (in seconds) and error rates for data communication across different floors in the NANO building. Transmission times are generally consistent, ranging from 39.91 seconds to 40.74 seconds on most floors, with a notable increase at floor 9 (40.56 seconds) and a dramatic spike at floor 10 (586.01 seconds). The error rates also vary, with most floors showing error rates between 0.00% and 0.91%, except for floor 9 (21.15%) and floor 10 (43.33%). The average transmission time is 94.78 seconds, with an average error rate of 6.68%. These results suggest that while transmission is relatively stable across most floors, significant interference occurs on the higher floors, particularly on floor 10, where both transmission time and error rate increase substantially. This increase in transmission time on higher floors is likely due to a combination of greater distance, the density of concrete materials, and interference from other HT signals, which all contribute to signal degradation and longer transmission delays.

IV. CONCLUSION

This research designed and tested a telemetry system for remote monitoring of renewable energy production, specifically for wind turbines and photovoltaic arrays. The system showed strong performance, with transmission times typically around 40 seconds for distances up to 250 meters. Transmission quality declined at greater distances, such as 500 meters, with an average error rate of 7.55%. This decrease in quality is due to signal attenuation and interference from other wireless signals, such as Wi-Fi and Bluetooth.

The system encodes data into an audio signal at 700 Hz, with an average transmission time of 40.21 seconds per data set. While suitable for periodic updates, this delay could be too slow for applications requiring rapid decision-making, such as fault detection. Testing across different channels showed average transmission times of 42.64 seconds, with error rates ranging from 0.00% to 2.98%, indicating stable performance in radio communication.

While the system is adequate for real-world applications, interference and signal degradation remain challenges. Improvements such as higher-gain antennas, signal repeaters, or alternative frequency bands could enhance performance. Adaptive transmission strategies may also improve reliability in challenging environments.

ACKNOWLEDGMENT

The Authods like to express their sincere gratitude to the Research Centre for New and Renewable Energy Engineering, Universitas Airlangga for providing the necessary support and resources that contributed to the completion of this research. Their valuable insights and technical guidance have been instrumental in shaping the outcomes of this study.

REFERENCES

[1] J. H. Ortiz, J. F. C. Garcia, O. I. Khalaf, F. V. Varela, P. J. B. Baron, and J. H. G. Atehortua, “Development of a Module for Measuring Electrical Variables in Power Transformers Based in IoT, to Manage and Monitoring by Telemetry Mechanism,” *Journal on Internet of Things*, vol. 3, no. 2, pp. 53–63, 2021, https://doi.org/10.32604/jiot.2021.014736.

[2] H. Abdillah, A. N. Afandi, M. Zainul Falah and A. Firmansah, "Solar Energy Monitoring System Design Using Radio Frequency for Remote Areas," *2020 International Conference on Smart Technology and Applications (ICoSTA)*, pp. 1-6, 2020, https://doi.org/10.1109/ICoSTA48221.2020.1570613859.

[3] C. M. Coman, A. Florescu, and C. D. Oancea, “Improving the Efficiency and Sustainability of Power Systems Using Distributed Power Factor Correction Methods,” *Sustainability*, vol. 12, no. 8, p. 3134, 2020, https://doi.org/10.3390/su12083134.

[4] B. N. Alhasnawi and B. H. Jasim, “A new internet of things enabled trust distributed demand side management system,” *Sustainable Energy Technologies and Assessments*, vol. 46, p. 101272, 2021, https://doi.org/10.1016/j.seta.2021.101272.

[5] N. M. Khoa, L. Van Dai, D. D. Tung, and N. A. Toan, “An advanced IoT system for monitoring and analysing chosen power quality parameters in micro-grid solution,” *Archives of Electrical Engineering*, vol. 70, no. 1, pp. 173-188, 2024, https://doi.org/10.24425/aee.2021.136060.

[6] A. H. A. AL-Jumaili, R. C. Muniyandi, M. K. Hasan, M. J. Singh, J. K. S. Paw, and M. Amir, “Advancements in intelligent cloud computing for power optimization and battery management in hybrid renewable energy systems: A comprehensive review,” *Energy Reports*, vol. 10, pp. 2206–2227, 2023, https://doi.org/10.1016/j.egyr.2023.09.029.

[7] O. Munoz *et al*., “Development of an IoT smart energy meter with power quality features for a smart grid architecture,” *Sustainable Computing: Informatics and Systems*, vol. 43, p. 100990, 2024, https://doi.org/10.1016/j.suscom.2024.100990.

[8] N. Sushma, H. N. Suresh, J. M. Lakshmi, P. N. Srinivasu, A. K. Bhoi and P. Barsocchi, "A Unified Metering System Deployed for Water and Energy Monitoring in Smart City," *IEEE Access*, vol. 11, pp. 80429-80447, 2023, https://doi.org/10.1109/ACCESS.2023.3299825.

[9] N. Sushma, H. N. Suresh, L. J. Mohana, and K. B. Santhosh Kumar, “Experimental investigation on wireless integrated smart system for energy and water resource management in Indian smart cities,” *Results in Engineering*, vol. 23, p. 102687, 2024, https://doi.org/10.1016/j.rineng.2024.102687.

[10] M. Güçyetmez and H. S. Farhan, “Enhancing smart grids with a new IOT and cloud-based smart meter to predict the energy consumption with time series,” *Alexandria Engineering Journal*, vol. 79, pp. 44–55, 2023, https://doi.org/10.1016/j.aej.2023.07.071.

[11] T. S. Rappaport, "Crucible Of Communications: How Amateur Radio Launched The Information Age And Brought High Tech To Life Part 2: Hams Bring Real-Time Communications To The World Invited Article," *IEEE Communications Magazine*, vol. 61, no. 11, pp. 10-23, 2023, https://doi.org/10.1109/MCOM.2023.10328195.

[12] M. R. Islam, S. Azam, B. Shanmugam and D. Mathur, "A Review on Current Technologies and Future Direction of Water Leakage Detection in Water Distribution Network," *IEEE Access*, vol. 10, pp. 107177-107201, 2022, https://doi.org/10.1109/ACCESS.2022.3212769.

[13] P. Fraga-Lamas, T. Fernández-Caramés, and L. Castedo, “Towards the Internet of Smart Trains: A Review on Industrial IoT-Connected Railways,” *Sensors*, vol. 17, no. 6, p. 1457, 2017, https://doi.org/10.3390/s17061457.

[14] L. Song, Y. Li, Z. Ding and H. V. Poor, "Resource Management in Non-Orthogonal Multiple Access Networks for 5G and Beyond," *IEEE Network*, vol. 31, no. 4, pp. 8-14, 2017, https://doi.org/10.1109/MNET.2017.1600287.

[15] A. Javan-Khoshkholgh and A. Farajidavar, "Simultaneous Wireless Power and Data Transfer: Methods to Design Robust Medical Implants for Gastrointestinal Tract," *IEEE Journal of Electromagnetics, RF and Microwaves in Medicine and Biology*, vol. 6, no. 1, pp. 3-15, 2022, https://doi.org/10.1109/JERM.2021.3084516.

[16] P. Kumar, S. K. Sharma, S. Singla, V. Gupta, and A. Sharma, “A review on mmWave based energy efficient RoF system for next generation mobile communication and broadband systems,” *Journal of Optical Communications*, vol. 45, no. 2, pp. 303–318, 2024, https://doi.org/10.1515/joc-2021-0159.

[17] W. Wang, J. Li, Y. He, X. Guo, and Y. Liu, “MotorBeat: Acoustic Communication for Home Appliances via Variable Pulse Width Modulation,” *Proceedings of the ACM on Interactive, Mobile, Wearable and Ubiquitous Technologies*, vol. 6, no. 1, pp. 1–24, 2022, https://doi.org/10.1145/3517255.

[18] L. Hernandez and E. Prefasi, "Analog-to-digital conversion using noise shaping and time encoding," *IEEE Transactions on Circuits and Systems I: Regular Papers*, vol. 55, no. 7, pp. 2026-2037, 2008, https://doi.org/10.1109/TCSI.2008.918003.

[19] M. R. Arvizo, J. Calusdian, P. E. Pace, K. B. Hollinger, “Robust symmetrical number system preprocessing for minimizing encoding errors in photonic analog-to-digital converters,” *Optical Engineering*, vol. 50, no. 8, p. 084602, 2011, https://doi.org/10.1117/1.3609801.

[20] H. Y. Teh, A. W. Kempa-Liehr, and K. I.-K. Wang, “Sensor data quality: a systematic review,” *Journal of Big Data*, vol. 7, no. 1, p. 11, 2020, https://doi.org/10.1186/s40537-020-0285-1.

[21] S. Adla, N. K. Rai, S. H. Karumanchi, S. Tripathi, M. Disse, and S. Pande, “Laboratory Calibration and Performance Evaluation of Low-Cost Capacitive and Very Low-Cost Resistive Soil Moisture Sensors,” *Sensors*, vol. 20, no. 2, p. 363, 2020, https://doi.org/10.3390/s20020363.